AIP | The Journal of Chemical Physics

Condensed phase ionic polarizabilities from plane wave density functional theory calculations

Robert J. Heaton, Paul A. Madden, Stewart J. Clark, and Sandro Jahn

Citation: The Journal of Chemical Physics **125**, 144104 (2006); doi: 10.1063/1.2357151
View online: http://dx.doi.org/10.1063/1.2357151
View Table of Contents: http://scitation.aip.org/content/aip/journal/jcp/125/14?ver=pdfcov
Published by the AIP Publishing

Condensed phase ionic polarizabilities from plane wave density functional theory calculations

Robert J. Heaton and Paul A. Madden[a)]
Chemistry Department, University of Edinburgh, Edinburgh EH9 3JJ, United Kingdom

Stewart J. Clark
Department of Physics, University of Durham, Durham DH1 3LE, United Kingdom

Sandro Jahn
GeoForschungsZentrum, Telegrafenberg, 14473 Potsdam, Germany

(Received 5 July 2006; accepted 30 August 2006; published online 11 October 2006)

A method is presented to allow the calculation of the dipole polarizabilities of ions and molecules in a condensed-phase coordination environment. These values will be useful for understanding the optical properties of materials and for developing simulation potentials which incorporate polarization effects. The reported values are derived from plane wave density functional theory calculations, though the method itself will apply to first-principles calculations on periodic systems more generally. After reporting results of test calculations on atoms to validate the procedure, values for the polarizabilities of the oxide ion and various cations in a range of materials are reported and compared with experimental information as well as previous theoretical results. © *2006 American Institute of Physics*. [DOI: 10.1063/1.2357151]

I. INTRODUCTION

The polarizability of an ion affects condensed phase properties in a number of ways. It determines the refractive index of a medium, and fluctuations in the polarizability density are responsible for Raman spectra. The polarization of an ion by its neighbors is recognized as an important contributor to the interaction energy and must be built into any transferable potential model. It has been known since the work of Mayer and Mayer[1] and the analysis of in-crystal polarizabilities by Tessman *et al.*[2] that the polarizabilities of anions in the condensed phase differ markedly from those of gas-phase ions; calculations show that for the F^- ion in crystalline LiF, for example, the polarizability is $6a_0^3$ compared to $16a_0^3$ for the isolated ion.[3] This is the consequence of the confining effect of the potential exerted by the charge distribution of neighbors on the electron density of the anion.[3,4] It follows that the anionic polarizabilities relevant to condensed phase studies do not have a single, well-defined value: the value will vary from material to material[5,6] and between the liquid and solid phases of a single material. It will be different for an ion on the surface compared to the bulk[7,8] and change as pressure is applied,[9,10] it will even vary from one instant to another as an ion undergoes thermal motions which distort its coordination environment (the effect responsible for the Raman scattering). In some cases, these differences will be sufficiently small that a single average polarizability will suffice to understand or model the material behavior but, increasingly, and particularly for the oxide ion where the isolated ion is unstable[11] and environmental effects on the polarizability are large, the need to have a systematic way of calculating the polarizability appropriate to a particular coordination environment is recognized. Similar considerations apply to the polarizabilities of ions dissolved in molecular solvents[12,13] and even to molecules in molecular media,[14] though here the environmental effects are weaker. The methods we describe below could also be applied to these cases.

Ab initio information on ionic polarizabilities in ionic materials has been obtained by performing quantum chemical style polarizability calculations on clusters embedded in a point charge lattice, in which the first neighbor shell around the ion of interest is explicitly included,[3] or by using spherical pseudopotentials to represent the confining potential.[4,6] These methods are confined to the study of ions in high symmetry sites in crystals. The cluster calculations lack generality because the calculations yield the polarizability of the whole cluster, from which the polarizability of the ion of interest must be extracted by uncoupling the multipole-induced-dipole interactions between all ions in the cluster which, especially in low symmetry clusters, requires knowledge of higher order multipole polarizabilities and hyperpolarizabilities. These problems are exacerbated by basis set superposition effects.[3,15] Nevertheless, in favorable cases, some information on the dependence of the polarizability on the identity of the neighboring ions, the number of coordinating ions and their geometrical arrangement,[9,16,17] on the polarizabilities of cations as well as anions,[18] and on the effect of taking an ion to surface sites[7] has emerged from the embedded cluster and pseudoenvironment calculations. This information has been used in the construction of polarizable interaction potentials,[19,20] in rationalizing the pressure dependence of the refractive index[9] and in calculating Raman spectra,[21] *inter alia*.

There is relatively little work on ions in molecular media or on solvent effects on the molecular polarizability. Jungwirth and Tobias[13] have examined solvent effects on ion

[a)]Electronic mail: paul.madden@ed.ac.uk

polarizability in aqueous solvents, and built this information into the polarizable potentials used in studying structure at the surface of aqueous electrolytes. They calculate only the electrostatic contribution to the confining potential from a point charge representation of the static charge distribution of solvating water molecules. They therefore bypass the calculation of multipole-induced dipole contributions to the cluster polarizability and the basis set superposition problems. Morita and Kato have proposed a more comprehensive scheme for dealing with molecular systems;[14] their calculations include both the electrostatic and exchange-repulsion effects and they remove the dipole-induced dipole contributions by appeal to a dielectric continuum model. They have shown how to systematically build molecular polarizable interaction potentials from *ab initio* calculations based on a variable charge scheme.

In this paper we propose an alternative, more readily applied method to obtain condensed phase polarizabilities from *ab initio* calculations, which can be applied to ions or molecules in arbitrary coordination environments. In this paper we will focus on the dipole polarizabilities of monatomic ions in ionic materials, but the method is easily generalized to deal with ions in an aqueous environment, molecular species, and with higher order polarizabilities. In subsequent work we will examine the dependence of the full tensorial character of the polarizability of an ion on the symmetry of its environment. We will show how information about the dependence of the polarizability on the immediate coordination environment in a system in thermal motion can be injected into polarizable interaction potentials which are more highly transferable than those in which a fixed polarizability is used[10] and we will also show how this information can be used to calculate Raman spectra on a first-principles basis.

The immediate intention is to extract polarizabilities from plane wave density functional theory (DFT) calculations of the type used to describe the electronic structure in the so-called *ab initio* molecular dynamics (MD) (AIMD) methods, a description which has been found appropriate to describe the interactions in many materials.[22] One motivating factor is to allow us to represent the polarization effects at the level implicitly present in the AIMD calculations, but in an explicit and more computationally efficient way through the use of polarizable interaction potentials. The use of DFT to calculate ionic polarizabilities merits further comment, as it is well known that anions are unbound in conventional DFT as a consequence of self-interaction effects which render the form of the exchange-correlation potential at large distances from the nucleus incorrect.[23,24] However, in the condensed phase, the confining environmental potential controls the asymptotic behavior of the wave function, at least for the densities normally encountered under ambient conditions, and the polarizabilities calculated from conventional DFT calculations agree well with those obtained from the quantum chemical methods.[25] At large lattice separations in model crystals, the predictions of the two methods begin to diverge, and it remains to be seen how reliable are the values of the polarizabilities obtained with the current method for ions at surface sites, etc, where the confining potential is relatively weak: it may be that an extension to use exact exchange is required for these cases.

We begin by outlining the method and explain how it is realized in practice by calculating the response of the electron density to an applied electric field. We validate the method by calculations on simple systems for which polarizabilities are known from experiment or calculations. We then apply the method to examine the polarizabilities exhibited by the oxide ion in various materials.

II. THE METHOD

The linear response of an ionic or molecular medium (i.e., one regarded as an assembly of closed-shell species) to an applied oscillating (optical frequency ω) electric field is characterized by the polarization $\mathbf{P}_\omega(\mathbf{r})$ which itself may be written in terms of the field-induced dipole moments of the individual ions (or molecules),

$$\mathbf{P}_\omega(\mathbf{r}) = \sum_i \mathbf{p}_\omega^i \delta(\mathbf{r} - \mathbf{r}^i). \tag{2.1}$$

It is useful to think about the response to an oscillating field at *optical* frequency ω to explain how the polarization of interest in the calculation of the polarizability could be distinguished, in principle, from that induced by intermolecular fields, and how, in an ionic material, we can neglect induced ionic currents. For an electronically insulating material, the induced dipole on each ion or molecule can be written in terms of the total (optical frequency) electric field which acts on it,[26]

$$\mathbf{p}_\omega^i(\{\mathbf{R}^N\}) = \boldsymbol{\alpha}^i(\{\mathbf{R}^N\}) \cdot \left[\mathbf{E}_\omega^0(\mathbf{r}^i) + \sum_{j \neq i} \mathbf{T}^{ij} \cdot \mathbf{p}_\omega^j(\{\mathbf{R}^N\}) \right]. \tag{2.2}$$

In this equation, we have introduced the dipole polarizability tensor $\boldsymbol{\alpha}^i(\{\mathbf{R}^N\})$ of ion i in the particular condensed phase configuration of ions denoted by $\{\mathbf{R}^N\}$; this configuration could be the instantaneous position of all the ions in a liquid, for example. The polarizability will depend on this configuration; the dependence could be weak, and this will be true in a molecular material held together by van der Waals forces, but for ions the dependence will be strong. Equation (2.2) also contains the applied field $\mathbf{E}_\omega^0(\mathbf{r}^i)$ which should be understood as the *external field*, that is the field which would be present at that point in space in the absence of all the ions which comprise the sample. This, rather than the field in the presence of the sample (the Maxwell field), is the appropriate field to introduce into an electronic Hamiltonian. Finally, $\mathbf{T}^{ij}$ is the dipole-dipole interaction tensor, $T_{\alpha\beta}^{ij} = \nabla_\alpha \nabla_\beta (r^{ij})^{-1}$, and this second term on the right-hand side of the equation is the reradiated field from the dipoles induced in all the other ions in the sample. In principle, higher order (optical frequency) multipoles contribute to this expansion but we will ignore them as in a uniform applied field the directly induced higher order multipoles on spherical atoms and ions will vanish.

In practice, we propose to apply this equation to the response of a sample of N ions in periodic boundary conditions to a uniform applied field. Consequently, we will replace the dipole-dipole tensor by its realization through an

Ewald sum[27] $\hat{\mathbf{T}}^{ij}$, and note that the sum over ions now includes the interaction of i with the images of all ions in the periodically replicated cells (including its own image, as indicated by the prime on the sum over ions in what follows). We can omit the ω subscript in what follows on the understanding that the dipoles are those induced due to the action of the external field.

Given a means of calculating the dipole moment on each ion induced by a uniform external field for some ionic configuration $\{\mathbf{R}^N\}$, we can invert Eq. (2.2) to determine the ionic polarizabilities. Consider the application of fields $\mathbf{E}^{0,\{x\}}$, $\mathbf{E}^{0,\{y\}}$, etc., along each Cartesian direction and denote by $\{\mathbf{p}^{i,\{x\}}\}_{i=1,N}$, $\{\mathbf{p}^{i,\{y\}}\}_{i=1,N}$, etc., the calculated values of the induced dipole moments. We can then obtain values for the total field at each ion $\mathbf{f}^{i,\{x\}}$, etc., for each applied field direction from

$$\mathbf{f}^{i,\{x\}} = \mathbf{E}^{0,\{x\}} + \sum_{j\neq i}{}' \hat{\mathbf{T}}^{ij} \cdot \mathbf{p}^{j,\{x\}}, \quad \text{etc.}, \tag{2.3}$$

which is conveniently evaluated from the electric field given by a dipolar Ewald sum with the dipoles set to $\{\mathbf{p}^{i,\{x\}}\}_{i=1,N}$ and the ion positions to $\{\mathbf{R}^N\}$. We may then obtain the polarizability tensor of ion i from

$$\boldsymbol{\alpha}^i(\{\mathbf{R}^N\}) = (\mathbf{F}^i)^{-1} \cdot \boldsymbol{\Pi}^i, \tag{2.4}$$

where $\mathbf{F}^i$ and $\boldsymbol{\Pi}^i$ are the 3×3 matrices,

$$F^i_{\alpha\beta} = f^{i,\{\beta\}}_\alpha, \qquad \Pi^i_{\alpha\beta} = p^{i,\{\beta\}}_\alpha, \tag{2.5}$$

and the subscripts refer to the Cartesian components of these vectors and tensors.

A. Induced molecular dipoles from plane wave DFT

We will obtain the individual ionic dipoles from a plane wave DFT calculation on a periodic system by transformation of the occupied optimum Kohn-Sham orbitals $\{\psi_\alpha\}_{\alpha=1,M}$ in the presence of an applied electric field to a maximally localized set of Wannier functions[28,29] $\{u_\alpha\}_{\alpha=1,M}$. In molecular and ionic (closed shell) systems, this transformation localizes a set of valence orbitals on each molecule and the molecular charge densities obtained from these orbitals have been shown to give excellent values for the molecular multipoles, as judged by their ability to reproduce the values obtained from more conventional quantum chemical methods on embedded clusters[28] and their use in discussing the charge density in interacting systems.[30] This procedure is, of course, not well-founded in theory: the best *a priori* justification which can be made is to note that the Wannier functions could be used to write down a valence bond representation of the total wave function of such a nonbonded (ionic) system in terms of localized, orthogonal functions, for which the total density would be the same as that which minimized the density functional. The multipoles obtained as above would be those which appear in an evaluation of the intermolecular electrostatic interaction energy with such a wave function.[31]

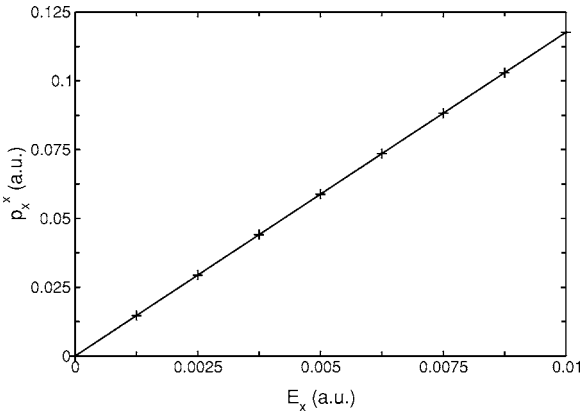

FIG. 1. Plot of $p_x^{\{x\}}$ against field strength (in atomic units) for an Ar atom in an 8 Å box.

We therefore require the Kohn-Sham orbitals from four electronic structure calculations, consisting of the unperturbed system and the system (at exactly the same atomic positions) in the presence of weak applied fields $\mathbf{E}^{0,\{x\}}$, $\mathbf{E}^{0,\{y\}}$, and $\mathbf{E}^{0,\{z\}}$. The molecular dipoles induced by these fields are calculated from the differences between the total molecular dipoles in the presence and absence of the fields. By performing calculations for several field magnitudes, we check that the induced dipoles are linear in the applied fields, but large enough to be outside the numerical noise. Methods for performing finite electric field calculations on periodic DFT calculations have been described.[32,33] In practice, for the small field strengths of interest, we have found it convenient to construct perturbed Kohn-Sham orbitals ψ^λ_α in the presence of a perturbation of strength λ (i.e., the strength of the external field in our context) by combining the unperturbed Kohn-Sham orbitals $\psi^{(0)}_\alpha$ with their first order corrections $\psi^{(1)}_\alpha$ as calculated with a linear response formalism.[34] Recalling that the first-order perturbed orbitals are mutually orthogonal and also orthogonal to *all* occupied unperturbed orbitals, themselves orthonormal, we may write

$$\psi^\lambda_\alpha = \frac{\psi^{(0)}_\alpha + \lambda\psi^{(1)}_\alpha}{1+\lambda^2\langle\psi^{(1)}_\alpha|\psi^{(1)}_\alpha\rangle}. \tag{2.6}$$

This linear response calculation was implemented in the CASTEP code[35] which we have used for the electronic structure calculations.

We need to perform four localization transformations on the KS orbitals to complete a calculation, which can be quite time consuming if there are many electrons in the system. We have found it useful to store the unitary matrix which effects the transformation for the unperturbed orbitals, and apply it to the electric-field-perturbed orbitals before completing their localization with a relatively small number of orbital rotations.[29]

III. TEST CASES

A. Neon and argon atoms

The method described above was used in some small test calculations carried out on neon and argon atoms. Figure 1 shows a plot of the dipole ($p_x^{\{x\}}$) induced on a single Ar atom

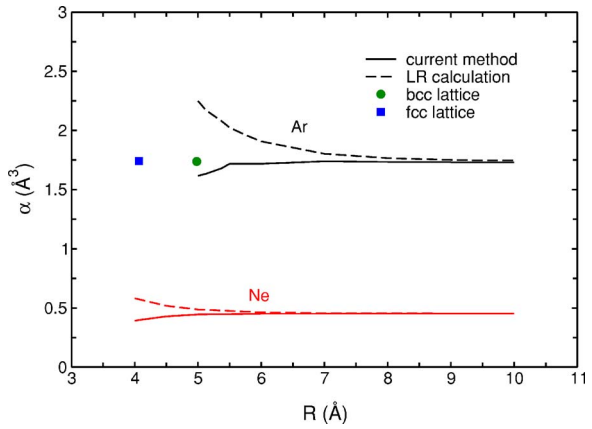

FIG. 2. The variation in the polarizability of a Ne atom and an Ar atom in a lattice as a function of the nearest neighbour separation R. The solid lines represents the results of the DFT calculations carried out on a simple cubic lattice, and the dashed line the results of the corresponding linear response calculation. The points shown with a circle and a square are the calculated Ar atom polarizabilities for 5.75 Å bcc and fcc lattices, respectively.

in an 8 Å periodically replicated, cubic cell, as the external field $\mathbf{E}^{0,\{x\}}$ is varied. We can see from this figure that the induced dipole is linear in the applied field. We have chosen a field strength of 0.005 a.u. well within this linear range but large enough to be the outside numerical noise in the linear response calculations, for all subsequent calculations. The calculations were performed with a plane wave cutoff of 1000 eV and only the Γ point was included in the Brillouin-zone (BZ) sampling scheme since our interest is in performing calculations with quite large simulation cells on insulating systems. These calculations were carried out using the Perdew, Burke Ernzerhof (PBE)[36] exchange-correlation functional and we used norm-conserving pseudopotentials created with this functional and optimized at the cutoff energy using the OPIUM program.[37]

Figure 2 shows the variation in the polarizability of single neon and argon atoms in periodically replicated cells of varying sizes (the full lines in the figure). Also shown (dashed line) is the polarizability of the whole cell extracted directly from the linear response calculation.[34] For small repeat distances of the periodic boundary conditions, the dipole-induced-dipole (DID) interactions between Ne and Ar atoms and their images in the periodically replicated simulation cell become significant: in effect, the atoms and their images constitute a simple-cubic lattice in which the nearest-neighbor separation (R) is the lattice parameter and each atom responds to the *local* field consisting of the external field plus the reradiated fields from all other atoms in the infinite lattice.[26] Consequently, the polarizability of the whole cell is a poor estimate of the polarizability of the individual atom; a local field factor should be applied. This fact has not been recognized in some previous works[34] where molecular polarizabilities have been calculated in periodic boundary conditions from the full cell polarizability. In the limit of large simulation cells, the local field reduces to the external field and the two sets of results converge on the same value of the atomic polarizability.

At still smaller cell sizes (interatomic separations), the calculated polarizabilities are seen to drop below their asymptotic values. A possible physical reason for this is that they are affected by overlap interactions between the electron density surrounding each atom and its image in neighboring cells. For a closed shell system, this overlap should reduce the value of the polarizability and this appears to accord with the findings. However, on further consideration, this decrease of the polarizability sets in at rather larger values of the interatomic separation R than would be expected for this effect at around 5.5 Å for Ar and 4.5 Å for Ne. For comparison, the van der Waals diameter of Ar is 3.4 Å and that of Ne is 2.9 Å; significant overlap effect should not occur until R is comparable with these values. An alternative explanation is that discrepancy arises because of the limitations of using only the Γ point in calculations where the periodic repeat distance is so small. In order to check this we have calculated the atomic polarizabilities in bcc and fcc arrangements for Ar in which the cubic cell lattice parameter is large enough at 5.75 Å for the simple cubic results to still agree with the large cell values (i.e., at the larger lattice constants the putative inadequacies of the BZ sampling are not apparent). The bcc and fcc lattices contain two and four atoms in the cubic cell and give interatomic Ar separations of 4.980 and 4.066 Å, respectively. These values are denoted by the additional points in Fig. 2; we see there is no reduction in the polarizability equivalent to that seen at interatomic distances below 5.5 Å for the simple cubic lattice. We conclude that the reductions in the polarizability seen for the simple cubic lattice are an artifact caused by using Γ-point calculations in very small cells. For the larger bcc and fcc lattices the polarizabilities are in good agreement with the values obtained for larger simple cubic lattice parameters. Since we intend to use the method to calculate the polarizabilities of ions in much larger cells, containing around 100 ions, the Γ-point approximation will be sufficient for subsequent calculations.

In Table I are shown the polarizabilities of the Ne and Ar atoms at the largest cell size appearing in Fig. 2. Also shown for comparison are the results on isolated atoms from more conventional quantum chemical style calculations[24] using several exchange-correlation functionals. Our PBE results are close to these accurate literature values, indicating that the current method gives results limited only by our choice

TABLE I. Atomic dipole polarizabilities (in Å^3) calculated using the current method are compared with literature values calculated using different exchange-correlation functionals (Ref. 24) and with the experimental values (Ref. 38).

Atom	Simple cubic	bcc	LDA	PBE	Expt.
Ne	0.452 59	0.452 76	0.452	0.442	0.396
Ar	1.730 80	1.734 47	1.780	1.728	1.640

of exchange-correlation functional. The calculated polarizabilities are consistently larger than the experimental values;[38] however, the PBE generalized gradient approximation seems to overestimate the polarizabilities somewhat less than the local density approximation (LDA) potential. This conclusion is in accord with previous work on molecular polarizability calculations within DFT.[24,39]

B. Ne–Ar dimer

We next calculated the polarizabilities of the atoms of a Ne–Ar dimer place in a 10 Å box. Such a dimer will have a permanent dipole moment and an anisotropic polarizability tensor, allowing a further test of the methodology. The Ne atom was placed in the cell at a position [0.4,0.4,0.4] and the Ar atom was placed at [0.6,0.6,0.6]. The distance between the atoms in the dimer was therefore 3.464 10 Å. From the linear response calculation, we can estimate this dimer polarizability tensor from the linear response result for the polarizability for the whole cell

$$\boldsymbol{\alpha}^{\mathrm{cell}} = \begin{pmatrix} 2.204\,72 & 0.033\,71 & 0.033\,71 \\ 0.033\,71 & 2.204\,72 & 0.033\,71 \\ 0.033\,71 & 0.033\,71 & 2.204\,72 \end{pmatrix}. \tag{3.1}$$

Recall that because of the DID interactions with the images (i.e., the local field effect), this is likely to overestimate the dimer polarizability, though in a 10 Å cell the effect should be small. The origin of the anisotropy in the dimer polarizability at this interatomic separation (beyond the sum of the atomic radii and therefore outside the range of overlap interactions) is DID interactions between otherwise undistorted (spherical) atoms.[40,41]

By application of the above procedure, which removes all DID effects, to the induced dipoles extracted from the same electronic structure calculations we obtain atomic polarizabilities of

$$\boldsymbol{\alpha}^{\mathrm{Ne}} = \begin{pmatrix} 0.452\,824 & -0.000\,758 & -0.000\,463 \\ -0.000\,771 & 0.452\,846 & -0.000\,746 \\ -0.000\,762 & -0.000\,728 & 0.452\,548 \end{pmatrix} \tag{3.2}$$

and

$$\boldsymbol{\alpha}^{\mathrm{Ar}} = \begin{pmatrix} 1.730\,687 & -0.003\,214 & -0.003\,205 \\ -0.002\,328 & 1.728\,334 & -0.002\,033 \\ -0.002\,622 & -0.002\,328 & 1.728\,913 \end{pmatrix}. \tag{3.3}$$

The individual atomic polarizabilities are seen to be almost isotropic (see below) as befits a spherical atom, with off-diagonal elements much smaller than the dimer polarizability, and the traces of these tensors are very close to the best estimates of the atomic polarizabilities appearing in Table I. By diagonalizing the dimer polarizability we obtain the polarizability of the dimer parallel and perpendicular to the intermolecular (Ne–Ar) axis: $\alpha^{\parallel}=2.272\,14$ Å^3 and $\alpha^{\perp}=2.171\,01$ Å^3. These values can be compared with values that we would expect for a pair of spherical atoms with only DID interactions,[41]

$$\frac{\alpha^{\parallel}}{R^3} = \frac{a+b+4ab}{1-4ab}, \qquad \frac{\alpha^{\perp}}{R^3} = \frac{a+b-2ab}{1-ab}, \tag{3.4}$$

where a and b are the polarizabilities of the Ne and Ar atoms, respectively, multiplied by R^{-3}, where R is the atomic separation. Taking the atomic polarizabilities to be the values listed in Table I, we obtain the molecular polarizabilities $\alpha^{\parallel}=2.262\,87$ Å^3 and $\alpha^{\perp}=2.146\,67$ Å^3, which compare well with the results of the linear response values; the differences are of the correct sign and size to be accounted for by the interimage DID (local field) effects.

Despite their small size, the off-diagonal elements of the atomic polarizability tensors merit further comment. Of course, these tensors should be symmetric and, furthermore, in this coordinate system, where the internuclear axis lies along the (111) direction of the simulation cell, all the off-diagonal elements should be equal, as should the diagonal elements. The departures from these expectations are due to numerical noise in our calculations of the atomic polarizabilities which arise from the convergence of the Wannier localization procedure used to isolate the induced dipoles on each atom. We have presented unvarnished results using the convergence criteria we have applied throughout the rest of the work which we have found lead to errors of the order of 0.5% of the dominant element of the polarizability tensor, as illustrated by the departures from the appropriate symmetry of atomic tensors quoted here. The noise can be reduced by forcing closer convergence in the localization, using finer grids to represent the Kohn-Sham orbitals, etc. While this is easily done on the small-scale test problems like these atomic problems, it becomes very expensive when applied to the many-ion configurations of interest in the work described below.

IV. CONDENSED IONIC MATERIALS

We next apply the method to the calculation of the polarizabilities of ions in oxide materials. In future work, we will examine the polarizability tensor of individual ions in instantaneously distorted coordination environments, but here we focus on the mean polarizability, for which experimental values and values from previous theoretical studies are available.

A. Comparison with the refractive index

The polarizability of the oxide ion is known to vary substantially from one condensed phase environment to another, and this effect is directly reflected in the measured values of the refractive index. The Lorenz-Lorentz[2,42] relationship expresses the connection between the ionic polarizabilities and the refractive index (n),

$$\frac{n^2-1}{n^2+2} = \frac{4\pi}{3}(\rho_+\alpha_+ + \rho_-\alpha_-). \tag{4.1}$$

Here ρ_+ and α_+ are the number density and mean polarizability of the cations, etc., respectively. This equation may be

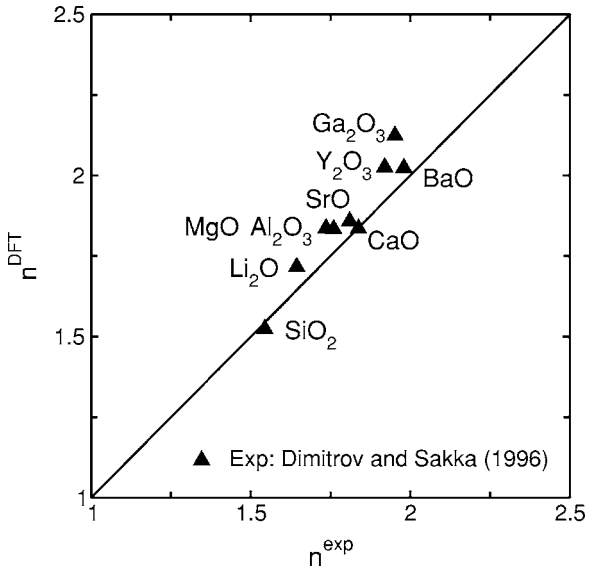

FIG. 3. This figure compares the DFT-calculated refractive indices (via the Lorentz-Lorenz relationship) with experimental data.

derived directly from Eq. (2.2) for a cubic lattice,[26] corrections are of order $(\alpha/R^3)^3$.

Figure 3 shows a comparison of the refractive indices predicted for various materials using polarizabilities obtained as described above from DFT calculations carried out on condensed phase configurations. The ionic configurations were derived from room temperature MD runs on the ground-state crystal structure using potentials of a type described elsewhere.[28] Each configuration contains 64–120 ions for each of the materials studied, the precise number depends on the crystal structure, and the values are given in the Appendix. Consequently, each calculation yields ~50 slightly different values for the trace of the polarizability tensor of the cation and oxide ion, the differences arise from the local coordination deformations caused by the thermal motion, and the results we describe below are averages over these values. These different structures place the oxide ion in a variety of coordination environments, eight coordinates in Li_2O, octahedral in MgO, SrO and BaO, two coordinates in SiO_2, and distorted four-coordinate sites in Al_2O_3, Y_2O_3, and Ga_2O_3. Because of the change of cation size, they also sample a wide range of nearest neighbor separations. Both factors have a substantial effect on the confining potential and (as we shall see) on the oxide ion polarizability and this contributes to the substantial increase in the refractive index with increasing cation size seen in the figure.

The calculations used plane wave cutoffs of 1000 eV, norm-conserving pseudopotentials and the LDA exchange-correlation functional. For the heavier cations, the electrons of the subvalence shell were explicitly included along with the valence shell of the oxide ions: for Li^+, Al^{3+}, and Si^{4+}, where the true cation polarizability is very small, the ion was fully pseudized and the calculated polarizability is zero. The details of these electronic structure calculations are given in the Appendix; the results are quite sensitive to the level of pseudization used as we will illustrate below.

Comparison of the experimental data for the refractive index and that obtained from the mean value of the traces of the *ab initio* polarizabilities combined with Eq. (4.1) suggests good agreement, especially for the materials with the smaller refractive indices. As the cation becomes larger, and also more polarizable, the tendency is for the calculations to slightly overestimate the experimental value. This tendency is consistent with the behavior of the LDA functional for molecular polarizabilities. We performed a calculation for Y_2O_3 where a PBE functional was used for the pseudopotential generation and in subsequent polarizability determination. The change of functional resulted in less than 1% reduction of the refractive index.

B. Comparison with individual ion polarizabilities

In order to trace the origin of this trend we can compare our calculations with polarizabilities of the individual ions. These have been extracted from the experimental data by using the Lorenz-Lorentz relationship and assuming that cation polarizabilities take fixed values, independent of the material in which they are found, whereas the oxide ion polarizability is allowed to be material dependent.[6,43] This assumption has been supported by comparisons between *ab initio* calculated free ion and in-crystal polarizabilities,[6] where for the most part groups I and II cations in high symmetry crystals have been examined. This approach has been critically examined very recently in an extensive survey of a wide range of materials by Shannon and Fischer.[5] Their analyses suggest that a better representation of refractive index data is achieved if the cation polarizability is allowed to increase above its free ion value in a coordination-number dependent way (the trend suggested by an examination of the environmental potential at a cation site[4]). We propose to examine this suggestion by a study of a wider range of materials in our future work. For the present, we make use of the "experimental" polarizabilities obtained with the constant cation polarizability assumption, but note that the separation of the experimentally measured refractive index into individual ionic polarizabilities does introduce a level of uncertainty.

1. Cation polarizabilities

In Fig. 4 we show the comparison between our calculated in-crystal cation values (the solid triangles in the figure) and the compilation by Dimitrov and Sakka,[43] where the cation polarizability is taken to be the value for a free ion.[44] The calculated values systematically lie below the quoted values for the polarizabilities of the heavier cations, especially Ba^{2+}. In order to trace the reason for these discrepancies, we have also calculated the polarizabilities of isolated cations by placing a single ion in a cell of 10 Å side and calculating its polarizability using the Wannier method with the same pseudopotentials and the same exchange correlation functional (LDA) as used to in the condensed-phase calculations. These values are shown by open triangles in the figure. The agreement between the free-ion cation polarizabilities quoted by Dimitrov and Sakka[43] and our calculated isolated ion values is remarkably good. This provides a clear vindication of the choice of functionals, pseudopotentials, and

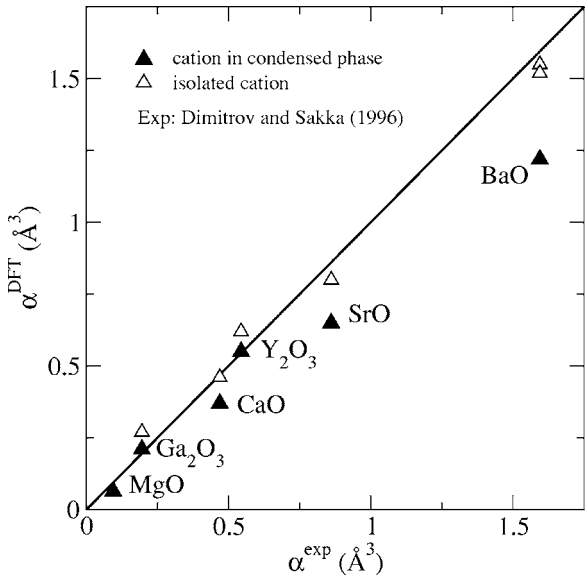

FIG. 4. Cation polarizabilities in some simple oxides. This figure compares the DFT calculated polarizabilities with those extracted from experimental data for a variety of structures in which the cations exhibit a range of polarizabilities.

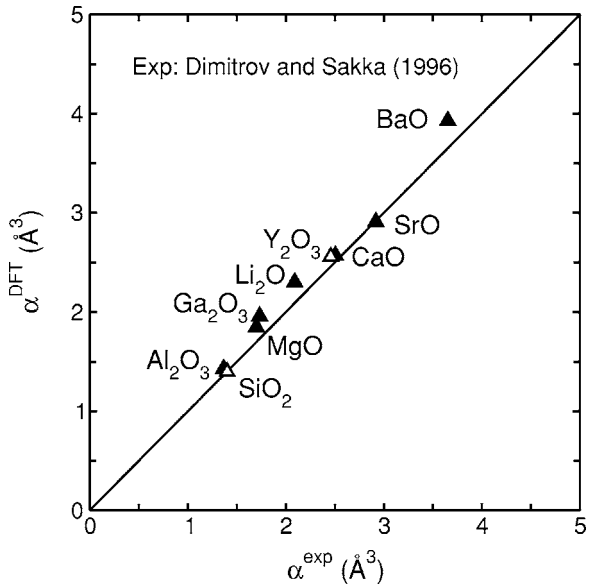

FIG. 5. Oxide ion polarizabilities in some simple oxides. This figure compares the DFT calculated polarizabilities with those extracted from experimental data for a variety of structures in which the oxide ion exhibits a range of polarizabilities.

method we have used. The surprising conclusion to emerge from the condensed-phase calculations then is that the in-crystal cation polarizabilities are *reduced* with respect to their gas-phase values, with the discrepancy becoming quite significant for the heavier cations. Nevertheless, as we shall see, the reduction is small compared to the oxide ion polarizabilities.

The isolated cation calculations were used to test the sensitivity of the results to several aspects of our DFT procedure. Using the OPIUM suite,[37] we generated a relativistic pseudopotential for Ba^{2+} using the method of Grinberg *et al.*[45] in order to compare with the nonrelativistic potential with the same pseudization scheme used in obtaining the results discussed above. These potentials were obtained so as to leave the $4d^{10}$ $5s^2$ $5p^6$ explicitly described in the DFT calculations for Ba^{2+}. The relativistic pseudopotential gives the same values for the atomic orbital energies as a full all-electron relativistic electronic structure calculation. We obtained values of 1.55 $Å^3$ using the nonrelativistic potential and 1.52 $Å^3$ with the relativistic one (both values are shown in Fig. 4). Secondly, we generated new pseudopotentials for Ba^{2+} (relativistic), and also several other cations, using the PBE exchange-correlation functional and the same pseudization schemes as in the Appendix. The calculated PBE value for the polarizability of the isolated Ba^{2+} ion was 1.53 $Å^3$, slightly larger than the LDA result above, and results for several other cations suggested that the difference between the LDA and PBE functionals for cation polarizabilities was very small. Finally we checked the sensitivity of the polarizability to the pseudization scheme by generating LDA potential so as to leave only the $5s^25p^6$ explicitly described in the DFT calculations for Ba^{2+}. This had a large adverse effect on the polarizability, increasing it to 1.72 $Å^3$. This may be a consequence of a poorer description of the "empty" 5*d* band in calculations with this potential rather than omission of the contribution to the polarizability of virtual electronic transitions out of the 4*d* band.

2. Oxide ion polarizabilities

In Fig. 5 we compare the oxide ion polarizabilities reported by Dimitrov and Sakka[43] with our values. The increase in the oxide polarizability with increasing cation size reflects the decrease in the strength of the confining potential in these materials. We can see that the calculated oxide polarizabilities are in good agreement with the experimental values: all the points, except possibly BaO, lie very close to the line $\alpha^{\mathrm{DFT}}=\alpha^{\mathrm{exp}}$ (which has been drawn as an aid for the eyes). In making the comparison, we should bear in mind that the experimental values have been extracted from the refractive index with the assumption that the cation polarizability is equal to the free ion value, whereas our calculations described in the last section suggest that smaller values should be used. This would result in small increases in the experimental oxide ion polarizabilities and bring about a systematic improvement with our values, but it would still leave them slightly higher. If we use our calculated in-crystal Ba^{2+} polarizability to extract an oxide ion value from the refractive index we find that the calculation overestimates the experimental value by about 0.15 $Å^3$. For BaO the confining potential is weakest because of the large size of the Ba^{2+} ion and the discrepancy may reflect the first signs of the deficiencies of DFT for calculating anion polarizabilities when the ions are in weak confining potentials which were detailed in Ref. 25.

Overall, we do not believe that the comparisons which are possible with the experimental data suggest any fundamental limitation of our method for extracting ionic polarizabilities from condensed phase electronic structure calculations *per se*. The comparisons with experiment are limited, on the one hand, because of the assumptions necessary to

extract individual ion polarizabilities from the measurable refractive index: on the other hand, we must use the Lorenz-Lorentz relationship to obtain the refractive index from the calculated values and the errors may be significant for high polarizability densities and nonpublic crystals. It may be possible to obtain accurate local-field factors numerically in future work and make the comparison with the refractive index more precise.

C. The coordination dependence of the oxide polarizability in MgO

To obtain *transferable* descriptions of the interactions in oxide materials, applicable to different phases and over a wide range of densities, it is important to allow for the dependence of the polarizability of the oxide ion on coordination number and on nearest neighbor separations. We have carried out a detailed study of the average polarizabilities predicted for the ions in MgO, in the rocksalt (B1), cesium chloride (B2), and zinc-blende (B3) structures at a variety of lattice parameters. These crystal structures contain six-, eight-, and four-coordinate oxide ions, respectively. Studies of the variation in polarizability of the oxide ion in MgO for these structures have been carried out by Pyper and Popelier[16] and Pyper[17] using Hartree-Fock (HF) *ab initio* techniques, and these results can be compared with those of the current method. In Pyper's calculations the confining effect of the coordination shell is represented by a spherical pseudopotential and only the electrons associated with the oxide ion are explicitly included in the calculation. Also, Domene *et al.*[25] examined the oxide ion polarizability in the B1 phase as a function of lattice parameter and contrasted the results obtained with various flavors of DFT with those obtained at the HF and HF plus Möller-Plesset level. These calculations are performed on clusters consisting of the ion of interest and its first coordination shell embedded in a point charge lattice. In this method it becomes difficult to isolate the polarizability of an individual ion when the ionic polarizabilities are large due to runaway values for the estimates of DID and basis set superposition errors. The HF results of Domene *et al.* agree well with Pyper's values for MgO in its equilibrium geometry, but their "best" results at MP2 level are larger which reflects a correlation contribution which is known to be positive and to increase in importance as the confining potential becomes weaker.[3]

In Fig. 6 we plot the average polarizability of the O^{2-} ions calculated using the current method *versus* the cation-anion separation R. The range of R values spans the values in the zero-pressure, equilibrium geometries for each of these phases (2.11, 2.24, and 2.02 Å for the B1, B2, and B3 structures, respectively). The B2 and B3 phases are not observed experimentally, so these R values are predicted by an *ab initio* force field[10] and included for guidance. The smaller R values become relevant for the behavior of the material under high pressure.[49] The polarizability calculations were carried out for the three crystal structures with the anions and cations being slightly displaced from their equilibrium positions in thermal motion at 300 K using this force field. The configurations used for the calculations each contained 50–100 atoms in periodic boundary conditions, and the calculations themselves used plane wave cutoffs of 1000 eV, norm-conserving pseudopotentials for the anions and cations (optimized at this cutoff energy), and the PBE exchange-correlation functional. The subvalence electrons of the Mg atom were included along with the valence shell of oxygen. Consequently, the representation of the coordination environment in these calculations should be better than in either the calculations of Pyper[17] or Domene *et al.*[25] since they include a full representation of the overlapping electron densities of all ions and there is no deterioration in the quality of the basis set as the lattice separation is increased. However, we are using the PBE exchange-correlation functional and, as detailed by Domene *et al.* and as seen above, this may be implicated in overestimation of the oxide polarizability, especially at large R where the confining potential becomes weak.

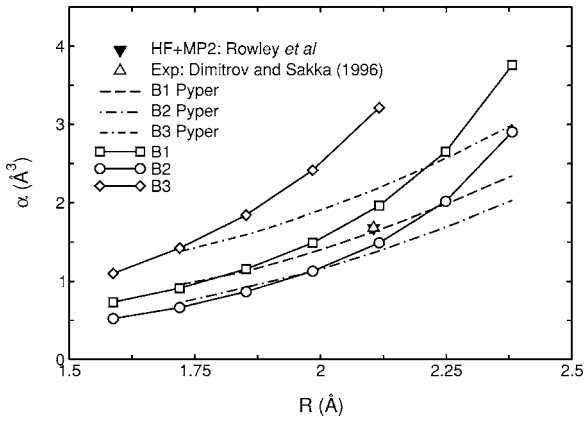

FIG. 6. Oxide anion polarizabilities for three MgO crystalline phases as a function of compression, compared with Hartree-Fock results by Pyper, and values extracted from experimental data for the rocksalt structure at the equilibrium lattice parameter. R is the nearest-neighbor separation in these structures.

As R is increased the strength of the confining potential is decreased and the anion polarizability rises. Furthermore, for a given cation-anion separation the confining potential decreases in strength in the sequence B2 > B1 > B3 because of the decreasing number of near-neighboring cations (eight, six, and four, respectively) and this is reflected in the increasing values of the polarizability in this sequence. In Fig. 6 we can see that all the $\alpha(R)$ curves rise steeply as R increases. This is the behavior that we would expect for an oxide ion which is unstable with respect to autoionization ($O^{2-} \rightarrow O^{-} + e^{-}$) by 8 eV (800 kJ mol^{-1}) in the gas phase[48] so that at large R the polarizability will be infinite. At small R, the results of the current method are in good agreement with the Hartree-Fock results of Pyper,[17] in accord with expectations from Ref. 25 on the performance of DFT calculations in strong confining potentials. In the physically important region near equilibrium (R_e=2.104 Å in the B1 structure), we also show the oxide polarizability extracted from experimental data[43] and the value obtained from Hartree-Fock plus Möller-Plesset calculations on clusters.[46] These values lie above the *ab initio* value of Pyper, but below the value predicted by the current calculations. At larger R, the polarizabilities predicted by the current method are greater than the Pyper values, the difference increasing with increasing R. In

part, this is because the Hartree-Fock values will progressively *underestimate* the true polarizability to an increasing extent as the confining potential becomes weaker: the correlation contributions to polarizability, ignored in the HF calculations, are positive and become more important in this regime.[11,47] Indeed, the gas-phase O^{2-} ion is stable in a restricted Hartree-Fock calculation, so that the large R behavior of the HF results is incorrect. However, the degree to which the DFT results exceed the HF ones is probably too large, reflecting, as also suggested by the results discussed above for BaO, the DFT deficiencies discussed in Ref. 25.

V. CONCLUSION

As judged by the comparison with experimental data and previous *ab initio* results, the method we have described gives good values for condensed-phase polarizabilities and captures the environmental effect on the anion polarizability very well, even for the notoriously difficult oxide ion. For cations, we find a small *decrease* in the in-crystal polarizability from the free ion value. The method is easy to apply and does not involve the construction of pseudopotentials to describe the environmental potential[16] or the unraveling of dipole induced dipole and basis set superposition errors in cluster calculations.[3,15] It can therefore be applied to ions in arbitrary condensed phase environments, such as the asymmetric instantaneous coordination environments encountered in the course of thermal motion in a liquid, where anisotropic elements of the polarizability will be induced alongside the trace. In future work we will exploit this capability to calculate Raman spectra and to build transferable models of ionic interactions.

The method rests on the use of the transformation of the Kohn-Sham orbitals to localized wannier functions which are then used to construct local charge densities from which the moments induced by an external field are extracted. This step cannot be justified rigorously, it was suggested by the success of using the Wannier analysis to examine charge densities in AIMD simulations. The quality of the present results provide further evidence to support the use of the Wannier analysis in this way, since we have been able to compare the results of the analysis with experimental values which bear directly on the values of the ionic dipoles themselves (rather than on the effect of the dipoles on intermolecular interactions). It would be possible to use the method on periodic electronic structure calculations which incorporate exact exchange and which avoid the fundamental limitations of DFT for negative ions: however, at present, no program is available which combines all the necessary technical elements.

ACKNOWLEDGMENTS

We are grateful to Leonardo Bernasconi and Philip Hasnip for the implementation of the Wannier localization in CASTEP. The electronic structure calculations were performed on the HPC(x) computer at the Daresbury Laboratory through the UK through EPSRC grant GR/S06233 and on the Bluegene(L) at the Edinburgh Parallel Computer Centre. The support of the HPC-Europa program, funded under the European Commission's Research Infrastructures activity of the Structuring the European Research Area program, Contract No. RII3-CT-2003-506079, is acknowledged.

APPENDIX: DETAILS OF THE ELECTRONIC STRUCTURE CALCULATIONS

The calculations were performed on condensed-phase configurations in periodic boundary conditions generated from room temperature MD simulations initialized from the low lying crystal structures of the materials concerned. This results in simulation cells containing the following number of ions: MgO, CaO, SrO, and BaO: 64 (8 atoms fcc$\times 2\times 2\times 2$), SiO_2: 72 (18 atoms in the orthorhombic cell$\times 2\times 1\times 2$), Li_2O: 96 (12 atoms in the cubic unit cell$\times 2\times 2\times 2$), Y_2O_3: 80 (bixbyite unit cell), and Al_2O_3 and Ga_2O_3: 120 (60 atoms in orthorhombic cell$\times 2\times 1\times 1$).

All the pseudopotentials used in these calculations were generated with OPIUM (Ref. 37) and were optimized at a plane wave energy cutoff of 1000 eV. They were generated with either a LDA or PBE exchange correlation functional, as described in the text, so as to match the functional used in the subsequent electronic structure calculation. The following shows the pseudization reference configurations used for each of the different atoms. For the oxides are included the lattice constants a (in angstroms) and cell angles α in degrees (when other than 90.0°) for each of the oxide calculations compared with the experimental values in square brackets: Ne: $2s^2 2p^6$; Ar: $3s^2 3p^6$; O: $2s^2 2p^4$; Li: $2s^{0.03}$, Li_2O: $a=4.556[4.574]$; Mg: $2s^2 2p^6$, MgO: $a=4.154[4.217]$; Ca: $3s^2 3p^6$, CaO: $a=4.796[4.8152]$; Sr: $3d^{10} 4s^2 4p^6$, SrO: $a=5.154[5.14-5.16]$; Ba: $4d^{10} 5s^2 5p^6$, BaO: $a=5.533[5.539]$; Al: $3s^{0.2} 3p^{0.1}$, Al_2O_3: $a=5.094[5.127]$ and $\alpha=55.45[55.3]$; Ga: $3d^{10} 4s^{0.2} 4p^{0.1}$; Ga_2O_3: $a=5.310[5.322]$ and $\alpha=55.96[55.82]$; Y: $4s^2 4p^{5.8} 4d^{0.4}$, Y_2O_3: $a=10.45[10.58-10.61]$; and Si: $3s^{0.4} 3p^{0.5} 3d^{0.1}$, SiO_2: $a=4.85[4.903]$ and $c=5.34[5.393]$.

[1] J. E. Mayer and M. G. Mayer, Phys. Rev. **43**, 605 (1933).
[2] J. R. Tessman, A. H. Kahn, and W. Shockley, Phys. Rev. **92**, 8902 (1953).
[3] P. W. Fowler and P. A. Madden, Phys. Rev. B **29**, 1035 (1984); J. Phys. Chem. **89**, 2581 (1985).
[4] G. D. Mahan and K. R. Subbaswamy, *Local Density Theory of Polarizability* (Plenum, London, 1990).
[5] R. D. Shannon and R. X. Fischer, Phys. Rev. B **73**, 23511 (2006).
[6] P. W. Fowler and N. C. Pyper, Proc. R. Soc. London, Ser. A **398**, 377 (1985).
[7] P. W. Fowler and P. Tole, Surf. Sci. **197**, 457 (1988).
[8] M. Wilson, J. Phys. Chem. B **101**, 4917 (1997).
[9] M. Wilson, P. A. Madden, P. Jemmer, P. W. Fowler, M. C. Monard, J. Bruno, and R. W. Munn, Mol. Phys. **96**, 1457 (1999).
[10] A. Aguado and P. A. Madden, Phys. Rev. B **70**, 245103 (2004).
[11] E. W. Pearson, M. D. Jackson, and R. G. Gordon, J. Phys. Chem. **88**, 119 (1984).
[12] G. Lamoureux and B. Roux, J. Phys. Chem. B **110**, 3308 (2006).
[13] P. Jungwirth and D. J. Tobias, J. Phys. Chem. B **106**, 6361 (2002); J. Phys. Chem. A **109**, 379 (2002).
[14] A. Morita and S. Kato, J. Chem. Phys. **110**, 11987 (1999); A. Morita, J. Comput. Chem. **23**, 1466 (2002).
[15] P. Jemmer, P. W. Fowler, M. Wilson, and P. A. Madden, J. Phys. Chem. B **102**, 8377 (1998).
[16] N. C. Pyper and P. Popelier, J. Phys.: Condens. Matter **9**, 471 (1997).
[17] N. C. Pyper, Mol. Phys. **95**, 1 (1998).
[18] C. Domene, P. W. Fowler, P. A. Madden, Jijun Xu, R. J. Wheatley, and M. Wilson, J. Phys. Chem. A **105**, 4136 (2001).

[19] P. A. Madden and M. Wilson, Chem. Soc. Rev. **25**, 339 (1996).
[20] A. Aguado, L. Bernasconi, and P. A. Madden, J. Chem. Phys. **118**, 5704 (2003).
[21] W. J. Glover and P. A. Madden, J. Chem. Phys. **121**, 7293 (2004).
[22] D. Marx and J. Hütter, *Ab Initio Molecular Dynamics: Theory and Implementation, Modern Methods and Algorithms of Quantum Chemistry*, NIC Series Vol. 1 (J. Grotendorst (Ed.), John von Neumann Institut fur Computing, Juelich, 2000), http://www.fz-juelich.de/nic-series/Volume1
[23] R. O. Jones and O. Gunnarssson, Rev. Mod. Phys. **61**, 689 (1989).
[24] J. J. A. van Gijsbergen, V. P. Osinga, O. V. Gritsenko, R. van Leeuwen, J. G. Snijders, E. J. Baerends, J. Chem. Phys. **105**, 3142 (1996).
[25] C. Domene, P. W. Fowler, P. Jëmmer, and P. A. Madden, Chem. Phys. Lett. **299**, 51 (1999).
[26] P. Mazur, Adv. Chem. Phys. **1**, 309 (1958).
[27] A. Aguado and P. A. Madden, J. Chem. Phys. **119**, 7471 (2003).
[28] A. Aguado, L. Bernasconi, S. Jahn, and P. A. Madden, Faraday Discuss. **124**, 171 (2003).
[29] G. Berghold, C. J. Mundy, A. H. Romero, J. Hütter, and M. Parrinello, Phys. Rev. B **61**, 10040 (2000).
[30] P. L. Silvestrelli, Phys. Rev. Lett. **82**, 3308 (1999).
[31] A. J. Stone, *The Theory of Intermolecular Interaction* (Clarendon, Oxford, 1996).
[32] I. Souza, J. Iniguez, and D. Vanderbilt, Phys. Rev. Lett. **89**, 117602 (2002).
[33] P. Umari and A. Pasquarello, Int. J. Quantum Chem. **101**, 666 (2005).
[34] K. Refson, P. R. Tulip, and S. J. Clark, Phys. Rev. B **73**, 155114 (2006).
[35] M. D. Segall, P. J. D. Lindan, M. J. Probert, C. J. Pickard, P. J. Hasnip, S. J. Clark, and M. C. Payne, J. Phys.: Condens. Matter **14**, 2717 (2002).
[36] J. P. Perdew, K. Burke, and M. Ernzerhof, Phys. Rev. Lett. **77**, 3865 (1996); **78**, 1396 (1997).
[37] N. J. Ramer and A. M. Rappe, OPIUM, http://opium.sourceforge.net/
[38] P. J. Leonard, At. Data Nucl. Data Tables **14**, 22 (1974).
[39] C. van Caillie and R. D. Amos, Chem. Phys. Lett. **291**, 71 (1998).
[40] K. L. Clarke, P. A. Madden, and A. D. Buckingham, Mol. Phys. **36**, 301 (1978).
[41] C. Domene, P. W. Fowler, P. Jemmer, and P. A. Madden, Mol. Phys. **98**, 1391 (2000).
[42] H. A. Lorenz, Ann. Phys. Chem. **9**, 641 (1880); **11**, 70 (1880).
[43] V. Dimitrov and S. Sakka, J. Appl. Phys. **79**, 1736 (1996).
[44] E. Kordes, Z. Phys. Chem. Abt. B **44**, 249 (1939).
[45] I. Grinberg, N. J. Ramer, and A. M. Rappe, Phys. Rev. B **62**, 2311 (2000).
[46] A. J. Rowley, P. Jemmer, M. Wilson, and P. A. Madden, J. Chem. Phys. **108**, 10209 (1998).
[47] P. W. Fowler and P. A. Madden, J. Phys. Chem. **89**, 2581 (1985).
[48] J. H. Harding and N. C. Pyper, Philos. Mag. Lett. **71**, 113 (1995).
[49] A. Aguado and P. A. Madden, Phys. Rev. Lett. **94**, 68501 (2005).